JACC: CARDIOVASCULAR IMAGING VOL. 6, NO. 11, 2013

ISSN 1936-878X/$36.00
PUBLISHED BY ELSEVIER INC. http://dx.doi.org/10.1016/j.jcmg.2013.05.017

Conductive Channels Identified With Contrast-Enhanced MR Imaging Predict Ventricular Tachycardia in Systolic Heart Failure

Lian-Yu Lin, MD, PHD,* Mao-Yuan M. Su, PHD,† Jien-Jiun Chen, MD,‡ Ling-Ping Lai, MD, PHD,* Juey-Jen Hwang, MD, PHD,* Chuen-Den Tseng, MD, PHD,* Yih-Sharng Chen, MD, PHD,§ Hsi-Yu Yu, MD, PHD,§ Wen-Yih I. Tseng, MD, PHD,†‖ Jiunn-Lee Lin, MD, PHD*

Taipei and Douliou, Taiwan

OBJECTIVES This study evaluated whether the conductive channel (CC) identified by late gadolinium enhanced–cardiac magnetic resonance (LGE-CMR) is associated with ventricular tachycardia (VT) in patients with systolic heart failure (HF).

BACKGROUND One recent study demonstrated that the CC formed by heterogeneous tissue within the core scar could be detected by LGE-CMR and that the CC is responsible for clinical VT. We hypothesized that the CC could help identify HF patients at risk for VT.

METHODS A total of 63 patients from a CMR database with left ventricular ejection fraction (LVEF) below 50% and with hyperenhancement on LGE-CMR were included. The cine and LGE images were analyzed to derive the LV function and scar characteristics, and to identify the CC. The outcomes, including VT, ventricular fibrillation (VF), and total mortality, were obtained by reviewing medical records.

RESULTS After a median 1,379 (interquartile range: 271 to 1,896) days of follow-up, 8 patients had VT/VF attacks and 14 patients died. Among the CMR-measured parameters, only the probability of identifying the CC by LGE-CMR was higher in patients with VT/VF than those without VT/VF (75.0% vs. 16.4%, $p < 0.001$). The probability of identifying the CC was also higher in the total mortality group than the survival group (50.0% vs. 16.3%, $p = 0.004$). The other LGE-CMR variables were not significantly different between the 2 groups. A univariate Cox regression model showed that CC identification was positively associated with VT/VF attacks (hazard ratio [HR]: 27.032, 95% confidence interval [CI]: 3.291 to 222.054, $p = 0.002$) and excess total mortality (HR: 4.766, 95% CI: 1.643 to 13.824, $p = 0.004$). The LVEF was inversely associated with VT/VF attacks (HR: 0.119, 95% CI: 0.015 to 0.977, $p = 0.048$) and excess total mortality (HR: 0.491, 95% CI: 0.261 to 0.925, $p = 0.028$) during follow-up.

CONCLUSIONS We demonstrated that CC identification using LGE-CMR can help identify HF patients at risk for VT/VF. (J Am Coll Cardiol Img 2013;6:1152–9) © 2013 by the American College of Cardiology Foundation

From the *Department of Internal Medicine, National Taiwan University Hospital, Taipei, Taiwan; †Department of Medical Imaging, National Taiwan University Hospital, Taipei, Taiwan; ‡Cardiovascular Center, National Taiwan University Hospital Yun-Lin Branch, Douliou, Taiwan; §Department of Surgery, National Taiwan University Hospital, Taipei, Taiwan; and the ‖Center for Optoelectronic Biomedicine, National Taiwan University College of Medicine, Taipei, Taiwan. This work was

Patients with congestive heart failure (HF) carry an additional risk of morbidity and mortality (1). It is of clinical importance to identify these high-risk patients because optimal medical and device therapy could substantially lower this risk (2,3). Recently, late gadolinium enhanced–cardiac magnetic resonance (LGE-CMR) has become a powerful tool for predicting cardiac events (4–6). In contrast to the precise left ventricular (LV) systolic function measurement offered by cine cardiac magnetic resonance (CMR), LGE-CMR has excellent sensitivity and specificity for detecting small myocardial scars and quantifying the core scar and border zone (5,6).

More recently, researchers have found that LGE-CMR could help identify the abnormal substrate for ventricular tachycardia, which could therefore facilitate the ablation procedure (7,8). Through image integration, LGE-CMR has been shown to detect ventricular tachycardia (VT)-associated scars that could not be identified by invasive electroanatomical voltage mapping (EAVM) (7). In 1 study, Perez-David et al. (8) showed that with computer-assisted visual identification, LGE-CMR could help detect the conductive channel (CC) within the scars. Through concomitant EAVM and electrophysiology analysis, the researchers further demonstrated that a significant amount of the CCs were critical isthmuses for VT (8).

In the present study, our goal was to investigate whether the CC identified by LGE-CMR could be used to predict risk for patients with systolic HF.

METHODS

Patient populations. This is a retrospective cohort study of an LGE-CMR database from 2004 to 2011. Patients with known renal dysfunction or estimated glomerular filtration rate <30 ml/min/1.73 m^2 were excluded from the CMR examination according to the American College of Radiology manual of contrast media. We surveyed the LGE-CMR database of the National Taiwan University Hospital and selected patients with left ventricular ejection fraction (LVEF) below 50% and with hyperenhancement on LGE-CMR. A total of 130 patients with LVEF <50% had a LGE-CMR examination. All patients had clinical symptoms and signs of congestive HF. We excluded 10 subjects with previous acute myocardial infarction (MI) whose LGE-CMR images were acquired within 3 months post-infarction. To investigate the prognostic value of LGE-CMR image parameters, we excluded 21 patients whose LV function deteriorated or recovered dramatically during follow-up (LVEF with over 15% of variation); the LVEF measured by various image modalities (echocardiography or radionuclide angiography) should have remained stationary in subsequent visits even after interventions such as percutaneous coronary intervention, coronary artery bypass graft, valve replacement or repair surgery, and cardiac-resynchronization therapy. Of the remaining 99 subjects, only 63 subjects with available LGE-CMR raw data were included for analyses. The basic demographics; cardiovascular risk factors, including hypertension, diabetes mellitus, dyslipidemia, and chronic kidney disease (CKD), defined as estimated glomerular filtration rate <60 ml/min, etiologies of impaired HF; medications of the included subjects; and other cardiovascular disease, such as ischemic stroke or peripheral arterial occlusive disease, were obtained by reviewing medical records. The outcomes, including malignant ventricular tachycardia and mortality etiologies, were also obtained by reviewing medical records or the National Health Institute database in Taiwan.

Magnetic resonance imaging. The study was performed on a 1.5-T magnetic resonance imaging system (Sonata, Siemens, Erlangen, Germany) with a 4-channel phased array torso coil. Cine CMR was first performed using a segmented balanced steady-state free precession gradient echo pulse sequence with a retrospective electrocardiographic R-wave gating. The scanning parameters were repetition time, 3.9 ms; echo time, 1.6 ms; flip angle, 70°; bandwidth, 977 Hz/pixel; slice thickness, 7 mm; gap, 3 mm; matrix size, 256 × 159; and pixel size, 1.3 mm × 1.3 mm. Multiple short-axis slices were prescribed from the mitral orifice to the LV apex. A total of approximately 10 to 12 short-axis slices were obtained, depending on cardiac size. For each slice level, patients were required to hold their breath for approximately 10 s. The true temporal resolution was 49 ms, and 30 cardiac phases were reconstructed for each slice level.

ABBREVIATIONS AND ACRONYMS

CC = conductive channel
CMR = cardiac magnetic resonance
EAVM = electroanatomical voltage mapping
HF = heart failure
LGE-CMR = late gadolinium enhanced–cardiac magnetic resonance
LV = left ventricle/ventricular
LVEF = left ventricular ejection fraction
MI = myocardial infarction
PSIR = phase-sensitive inversion recovery
SI = signal intensity
VF = ventricular fibrillation
VT = ventricular tachycardia

supported in part by the National Science Council, Taiwan (grant numbers: NSC-99-2314-B-002-116-MY3 and NSC-102-2314-B-002-087-MY2). The authors have reported that they have no relationships relevant to the contents of this paper to disclose. Drs. L-Y Lin and Su contributed equally to this work.

Manuscript received November 9, 2012; revised manuscript received May 3, 2013, accepted May 6, 2013.

The LGE-CMR image study was performed by slow infusion of a gadolinium-based contrast agent (Magnevist, Berlex Laboratories, Wayne, New Jersey) through the left antecubital vein; the dose was 0.2 mmol/kg body weight. Ten minutes after contrast medium injection, LGE images were acquired in the same short-axis planes as those used for cine images by using an electrocardiographic R-wave–triggered, phase-sensitive inversion recovery (PSIR) prepared segmented fast gradient echo pulse sequence (9). The scanning parameters were inversion time (TI)/repetition time/echo time, 250 ms/9.6 ms/4.2 ms; flip angle, 25°; bandwidth, 130 Hz/pixel; slice thickness, 7 mm; gap, 3 mm; matrix size, 256 × 192; and pixel size, 1.37 mm × 1.37 mm. We acquired LGE-CMR images using PSIR sequence with a fixed TI of 250 ms. The PSIR sequence takes into account the polarity of the z-magnetization, and so the contrast between the normal myocardium and the scar is kept relatively stable despite the mismatch of the TI with the null point of the normal myocardium (10). This feature allows us to complete the acquisition of the LGE-CMR images quickly, without spending time on adjusting the TI.

Image analysis. LV FUNCTION AND MASS ANALYSIS FROM CINE CMR. Detailed procedures regarding LV function and mass analysis have been described elsewhere (11). Briefly, the endocardial and epicardial contours of the LV in the short-axis view were determined at each slice level by a user-interface graphics program, which used a gray-level autocontouring algorithm provided by MATLAB version 7.9 (MathWorks, Natick, Massachusetts). The area enclosed by each contour was computed. The LV volumes for each time point were then determined by Simpson's rule to obtain the volume–time curve of the LV. This is equivalent to the sum of the areas of the corresponding slice levels multiplied by the slice thickness plus gap. The end-diastolic volume and end-systolic volume were assessed from the maximal and minimal values of the volume–time curve. These values were used to compute the LVEF. LV mass was computed as the difference between LV epicardial volume at end-diastole and end-diastolic volume, multiplied by the density of the myocardium, which is 1.05 g/ml.

QUANTIFICATION OF THE CORE SCAR AND GRAY ZONE. The infarct and remote zones were determined on LGE-CMR images for each patient. On the LGE images, the endocardial and epicardial contours were manually traced to define the LV wall. The infarct zone was defined as the sector of the LV wall that contained hyperenhancement of any transmurality. The remote zone was defined as the remaining portion of the LV wall that did not contain hyperenhancement. In the infarct zone, a pixel was counted as the core scar if its signal intensity (SI) was higher than 3 SD above the average SI of the remote myocardium, and it was counted as the gray zone if the SI was between 2 and 3 SD above the average SI of the remote zone (12). The volumes of the core scar and of the gray zone were quantified based on the Simpson's rule: volume = (summation of the interested areas of all short-axis slices) × (slice thickness + gap). The volumes were normalized by an individual's total LV mass volume and are expressed in terms of percentages.

IDENTIFICATION OF THE CONDUCTIVE CHANNELS. The CC in the ventricular wall was identified and defined according to a previous study (8). Two investigators (L.Y.L. and M.Y.S.), who were blinded to the outcomes, analyzed the data. A custom-developed MATLAB program was used to create a

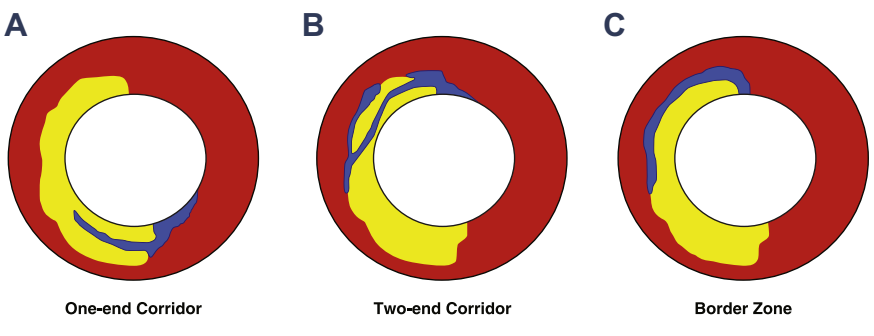

Figure 1. Illustration of a CC

A conductive channel (CC) is considered if a corridor of the heterogeneous tissue **(blue zone)** penetrates the scar **(yellow zone)** with its 1 end, a 1-end corridor **(A),** or 2 ends, a 2-end corridor **(B),** connecting to the normal myocardium **(red zone)**. If the gray zone **(blue zone)** surrounds the scar without penetration into the scar **(C)**, it is not considered a CC.

computer-assisted image that was derived by subtracting the difference of the areas between regions with an SI over 2 SD and regions over 3 SD for each short-axis slice. (8). As illustrated in Figure 1, by visually reviewing each subtraction image, a CC is considered if a corridor of the heterogeneous tissue (blue zone) penetrates the scar (yellow zone) with its 1 end (Fig. 1A) or 2 ends (Fig. 1B) connecting to the normal myocardium (red zone). If the gray zone surrounds the scar without deep penetration into the scar (Fig. 1C), it is not considered a CC. Figures 2A and 2B are LGE-CMR images that were obtained from 2 patients with a CC in the infarct zones. Figure 2C shows images of a patient without a CC. The presence of a CC was only accepted if both investigators independently agreed on the outcome. In this study, we used the phase image of the PSIR as opposed to the magnitude image to quantify the myocardial scar and CC. The benefits of the reconstructed image include reduction of sensitivity in B1 field inhomogeneity, increased tolerance of TI, background noise reduction, and nearly complete magnetization recovery (9).

Statistics. The normality of the variables was tested by the Shapiro-Wilk test. Continuous variables with normal distribution are expressed as means ± SD, whereas those that were not normally distributed are reported as medians and interquartile ranges (25% to 75%). Categorical variables were expressed as percentages. The demographics, etiology for HF, medication usage, and image variables were compared between patients with different outcomes by using the Student *t* test for normally distributed continuous variables and by using the Mann-Whitney *U* test for those that were not normally distributed. Categorical variables between patients with different outcomes were compared by the Fisher exact test. The predictors for outcomes, which included VT, ventricular fibrillation (VF), and total mortality, were analyzed by a univariate Cox regression model. The hazard ratio (HR) was calculated for each LGE-CMR variable. The presence of CC was entered as a categorical variable (yes or no). The LVEF, the LV mass, the core scar, and the gray zone were also entered as categorical variables by using their median values as cut points

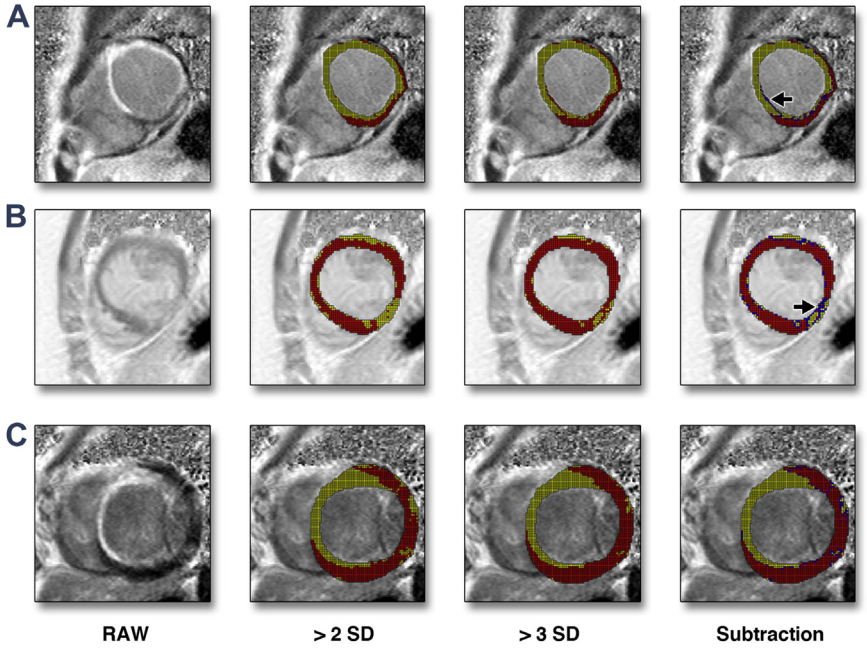

Figure 2. Computer-Assisted Visual Identification of a CC in LGE-CMR Images

The **first column** (RAW) shows the late gadolinium enhancement–cardiac magnetic resonance (LGE-CMR) images. The **second column** (>2 SD) shows the division of the left ventricular myocardium into the **yellow region**, which has a signal intensity (SI) higher than the mean +2 SD threshold in the remote myocardium. The **red region** has a SI lower than this threshold. The **third column** (>3 SD) shows the division using the threshold of the mean +3 SD in the remote myocardium. The **fourth column** (Subtraction) shows 3 divisions of the myocardium; the **yellow region** has a SI > the mean +3 SD, the **red region** has a SI < the mean +2 SD, and the **blue region** has a SI between the mean +2 SD and the mean +3 SD. **A** and **B** show LGE-CMR images with conductive channels (CCs) **(arrows)**, and **C** shows images without CCs. A CC was defined as a corridor of the gray zone **(blue zone)** surrounded by the scar with its end(s) connecting to the normal myocardium.

(≥ or < median values). For Kaplan-Meier survival analysis, patients were divided into 2 groups that were stratified according to the existence of the CC. Between-group differences in survival were tested by log-rank statistics. A p value <0.05 was considered statistically significant.

RESULTS

A total of 63 patients, age 27.3 to 83.3 years, were included. Of this total, 14 patients were women and 49 were men. The median number of follow-up days was 1,379 (interquartile range, 271 to 1,896) days. Three cases were lost during follow-up. During the follow-up period, 8 patients had VT/VF attacks, and 14 patients died. Among the 14 mortalities, 6 patients died of ventricular tachycardia, 4 died of congestive HF, 2 died of severe sepsis, and 2 died of respiratory failure. The basic demographics, risk factors, etiology for HF, comorbidities, medication usage, CMR image parameters, and the incidence of new stable angina or acute coronary syndrome (ACS) during follow-up between patients with and without VT/VF are summarized in Table 1. As shown in Table 1, patients with VT/VF were more likely to have CKD with borderline significance (62.5% vs. 25.9%, p = 0.050). Among the LGE-CMR image parameters, only the probability of identifying the CC by LGE-CMR was higher in patients with VT/VF (75.0% vs. 16.4%, p < 0.001). Other statistically insignificant variables between the 2 groups included age, sex, incidence of hypertension, diabetes mellitus, dyslipidemia, old MI, other cardiovascular diseases, etiologies for HF, the percentage of antiplatelet, beta-blocker, and angiotensin-converting enzyme inhibitor/angiotensin receptor blocker usage, LVEF, LV mass, the percentages of the core scar and gray zone, and the incidence of new stable angina or ACS during follow-up.

Table 1. Basic Demographics, Risk Profile, Medication Use, and CMR Image Parameters in Subjects With and Without VT/VF

	VT/VF (n = 8)	Free of VT/VF (n = 55)	p Value
Age, yrs	59.3 ± 15.2	60.6 ± 11.7	0.744
Male	75.0	78.2	1.000
Risk factors			
HTN	25.0	27.3	1.000
DM	12.5	34.5	0.418
Dyslipidemia	25.0	20.0	0.665
CKD	62.5	25.9	0.050
Comorbidities			
Old MI	62.5	32.7	0.129
Other CVD	0.0	5.5	1.000
Etiologies for HF			
Ischemic CMP	87.5	87.3	0.581
Dilated CMP	12.5	9.1	1.000
Valvular heart disease	0.0	3.6	1.000
Medications			
Antiplatelet	25.0	34.5	0.708
Beta-blocker	37.5	60.0	0.272
ACEI/ARB	37.5	60.0	0.272
CMR parameters			
LVEF, %	31.0 (25.3–33.8)	36.0 (26.0–44.0)	0.457
LV mass, g	167.3 ± 59.1	157.8 ± 44.0	0.589
LVEDV, cm^3	172.6 (114.8–222.3)	179.0 (148.7–250.5)	0.393
Core scar	43.9 ± 18.3	34.3 ± 15.3	0.109
Gray zone	12.0 ± 2.9	12.9 ± 2.7	0.189
Patients with CC	75.0	16.4	<0.001
Other outcomes during follow-up			
New stable angina	12.5	9.1	0.573
New ACS	0.0	3.6	1.000
Follow-up, days	137 (47–1,117)	1,508 (456–1,950)	0.016

Values are mean ± SD, %, or median (interquartile range).
ACEI/ARB = angiotensin-converting enzyme inhibitor/angiotensin receptor blocker; ACS = acute coronary syndrome; CC = conductive channel; CKD = chronic kidney disease; CMP = cardiomyopathy; CMR = cardiovascular magnetic resonance; CVD = cardiovascular disease; DM = diabetes mellitus; HF = heart failure; HTN = hypertension; LV = left ventricular; LVEDV = left ventricular end-diastolic volume; LVEF = left ventricular ejection fraction; MI = myocardial infarction; VF = ventricular fibrillation; VT = ventricular tachycardia.

The basic demographics, risk factors, HF etiology, comorbidities, medication usage, CMR variables, and the incidence of new stable angina or ACS during follow-up between mortality and survival groups are summarized in Table 2. Among the variables, the incidence of CKD (57.1 vs. 22.9, p = 0.022), old MI (64.3% vs. 28.6%, p = 0.026), and the probability of the identification of the CC (50.0% vs. 16.3%, p = 0.004) were significantly higher in the mortality group. Other variables were not statistically significant between the mortality and survival groups.

The HR of each CMR image variable in predicting different outcomes is shown in Table 3. The median values for LVEF, LV mass, core scar, and gray zone are 37.5%, 148.5 g, 33.41%, and 12.9%, respectively. Among the CMR image parameters, the identification of the CC was positively associated with VT/VF attacks during follow-up (HR: 27.032, 95% confidence interval [CI]: 3.291 to 222.054, p = 0.002). The LVEF (HR: 0.119, 95% CI: 0.015 to 0.977, p = 0.048) was inversely associated with VT/VF attacks. Other parameters, which included LV mass and percentages of the core scar and gray zone, were not significantly associated with VT/VF attacks. As for the prediction of total mortality, the identification of the CC (HR: 4.766, 95% CI: 1.643 to 13.824, p = 0.004)

and the LVEF (HR: 0.491, 95% CI: 0.261 to 0.925, p = 0.028) were also predictors for excess mortality.

Figure 3 shows the Kaplan-Meier survival curves for VT/VF attacks (Fig. 3A) and total mortality (Fig. 3B). Log-rank statistics showed that patients with a CC had a significantly poorer prognosis than those without a CC (p < 0.001 and p = 0.007 for VT/VF and total mortality, respectively).

DISCUSSION

Our results showed that among the LGE-CMR image parameters, only the presence of the CC and lower LVEF were significantly associated with VT/VF attacks and total mortality.

LGE-CMR has emerged as an important clinical tool in predicting cardiac events in patients with HF (5,6,12–18). Many studies have demonstrated that the extension of the scar measured by LGE-CMR is superior to traditional risk predictors such as LVEF and LV volumes in predicting future cardiac events (13–17). In the present study, we showed that the percentages of the core scar and gray zone are not associated with VT/VF attacks and total mortality. It is likely that the "quality" of the scar, such as tissue heterogeneity or presence of the CC, rather than the quantity plays a larger role in the generation of VT/VF.

Many previous reports have shown the importance of the scar heterogeneity, that is, the peri-scar gray zone in predicting cardiac events. These reports suggest that the residual peri-infarct myocardium might provide the substrate for arrhythmias and/or ischemia (5,6,12,14,18). In contrast to these previous studies, our data showed that the percentage of the gray zone is not a predictor for either VT/VF and total mortality. One possible explanation is that the criteria of SI to identify the core scar and the gray zone are different among studies. Another possibility is that the patients in the current analysis seldom (3.2% had new stable angina, and 9.5% had ACS) had any new ischemic episodes during follow-up. It is well known that revascularization of the ischemic regions could substantially reduce the incidence of ventricular arrhythmia in patients with ischemic cardiomyopathy (19,20). It is possible that a peri-infarct gray zone without ischemia is electrophysiologically more stable and is less likely to generate VT/VF. Finally, the critical site of VT/VF generation has been shown to be located predominately within the region of the core scar (8,21). This explains our main finding that the presence of the CC within the core scar is better than quantifying scar heterogeneity in predicting VT/VF attacks.

Human studies have shown that the slow conduction area or critical isthmus of the scar-related VT re-entrant circuit is composed of bundles of viable, but injured, myocytes embedded in the scar tissue (22,23). The heterogeneous tissue, although mainly located in the peri-scar region, is most likely more harmful when located within the core scar area, resulting in the formation of the so-called CC. The CC can now be identified invasively by endocardial voltage mapping and has become a standard procedure for scar-related VT ablation (24,25). In a recent cross-sectional design study, Perez-David et al. (8) showed that the CC could be identified noninvasively by computer-assisted

Table 2. Basic Demographics, Risk Profile, Medication Use, and CMR Image Parameters in Subjects With and Without Mortality

	Mortality (n = 14)	Survival (n = 49)	p Values
Age, yrs	62.7 ± 12.3	59.8 ± 12.1	0.438
Male	64.3	81.6	0.272
Risk factors			
HTN	35.7	24.5	0.498
DM	28.6	32.7	1.000
Dyslipidemia	21.4	20.4	1.000
CKD	57.1	22.9	0.022
Comorbidities			
Old MI	64.3	28.6	0.026
Other CVD	0.0	6.1	1.000
Etiologies for HF			
Ischemic CMP	100.0	87.8	0.182
Dilated CMP	0.0	10.2	0.323
Valvular heart disease	0.0	2.0	1.000
Medications			
Antiplatelet	42.9	30.6	0.522
Beta-blocker	42.9	61.2	0.240
ACEI/ARB	35.7	63.3	0.124
CMR parameters			
LVEF, %	31.4 (25.8–34.5)	36.0 (26.0–44.5)	0.679
LV mass, g	163.2 ± 45.8	157.9 ± 46.2	0.705
LVEDV, cm^3	172.6 (144.3–215.5)	179.0 (147.0–257.1)	0.566
Core scar	41.7 ± 18.0	33.7 ± 15.0	0.100
Gray zone	14.4 ± 4.0	10.7 ± 2.8	0.574
Patients with CC	50.0	16.3	0.004
Other outcomes during follow-up			
New stable angina	10.2	7.1	1.000
New ACS	7.1	2.0	0.398
Follow-up, days	81 (46–407)	1,542 (650–1,986)	<0.001

Values are mean ± SD, %, or median (interquartile range).
Abbreviations as in Table 1.

Table 3. Hazard Ratios and 95% CIs of the Univariate Cox Regression Model With VT/VF Attacks and Mortality as Outcome

	VT/VF (n = 8)	Total Mortality (n = 14)
LVEF	0.119 (0.015–0.977) p = 0.048	0.491 (0.261–0.925) p = 0.028
LV mass	1.657 (0.396–6.941) p = 0.489	0.918 (0.515–1.637) p = 0.771
Core scar	3.751 (0.753–18.677) p = 0.106	1.134 (0.628–2.047) p = 0.677
Gray zone	0.251 (0.050–1.249) p = 0.091	0.615 (0.337–1.122) p = 0.113
Presence of CC	27.032 (3.291–222.054) p = 0.002	4.766 (1.643–13.824) p = 0.004

Abbreviations as in Table 1.

visual identification of the LGE-CMR image. By concomitant EAVM and electrophysiology study, the authors also showed that each CC identified by noninvasive method corresponded to a similar channel detected by EAVM, and a majority of the channels were related to VT critical isthmuses (8). In the present study, we further demonstrated that CC could also help identify patients at risk of VT/VF. Furthermore, in the present study, 6 of 14 patients died of VT/VF; therefore, the CC also became a predictor for total mortality.

Study limitations. First, the study population is small, and the study cohort is retrospective. Second, because we did not perform EAVM for our patients, there were no invasive data to validate the CC identified by LGE-CMR. Third, in this study, all of the LGE images were acquired with an inversion recovery prepared segmented 2-dimensional (2D) turbo fast low angle shot sequence, not the 3-dimensional sequence. The LGE images acquired with the 2D sequence only allows us to identify corridors within each 2D image. We cannot perform 3-dimensional reconstruction of the LGE images and examine the vertical corridors as Perez-David et al. (8) did. Also, each LGE-CMR slice image was 3 mm apart, which may not be close enough to detect any potential CC located between the slices. However, the slices were uniformly distributed, and the coverage reached up to 70% of the whole LV myocardium. The impact of underestimating CC or scar should be insignificant. Despite this limitation, our results show that the conductive channels identified on 2D images still constitutes a good predictor of ventricular tachycardia in patients with HF. Finally, the identification of the CC is sensitive to the definition of the SI thresholds of core scar and gray zone. The main reason for using a 3 SD threshold to identify the infarct zone is because the area produced by this threshold matches closely with what is shown on the LGE images by visual inspection. The optimal definition should be validated by invasive 3-dimensional EAVM.

CONCLUSIONS

We demonstrated that a CC identified in an LGE-CMR image can help identify patients at risk of VT/VF. Large-scale studies are needed to confirm whether this finding could guide the physicians to choose proper therapy (for example, an implantable

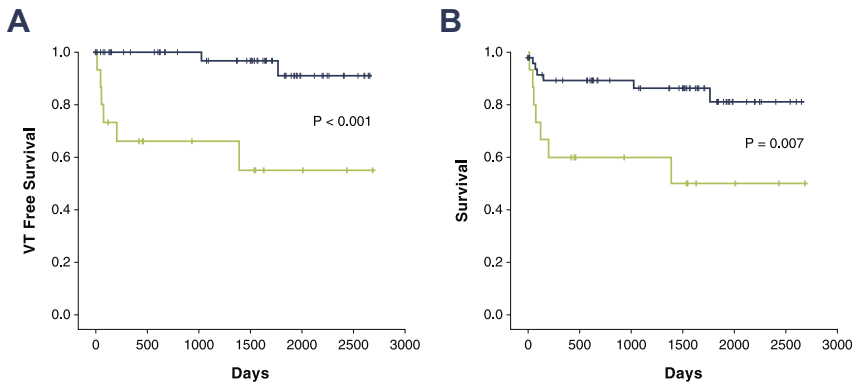

Figure 3. Kaplan-Meier Survival Curves and Log-Rank Statistics for VT/VF Attacks and Mortality

Statistics for ventricular tachycardia (VT)/ventricular fibrillation (VF) attacks **(A)** and mortality **(B)** are shown. The **green lines** represent patients with conductive channels, whereas the **blue lines** represent patients without conductive channels.

cardioverter-defibrillator) for their patients with HF.

Reprint requests and correspondence: Dr. Jiunn-Lee Lin, Department of Internal Medicine, National Taiwan University Hospital, No. 7, Chun-Shan S. Road, Taipei, Taiwan. *E-mail: jiunnlee@ntu.edu.tw.* OR Dr. Wen-Yih I. Tseng, Center for Optoelectronic Biomedicine, National Taiwan University College of Medicine, No. 1, Jen-Ai Road, Section 1, Taipei, Taiwan. *E-mail: wytseng@ntu.edu.tw.*

REFERENCES

1. Schocken DD, Arrieta MI, Leaverton PE, Ross EA. Prevalence and mortality rate of congestive heart failure in the United States. J Am Coll Cardiol 1992;20:301–6.
2. Moss AJ, Zareba W, Hall WJ, et al. Multicenter Automatic Defibrillator Implantation Trial II Investigators. Prophylactic implantation of a defibrillator in patients with myocardial infarction and reduced ejection fraction. N Engl J Med 2002;346:877–83.
3. Moss AJ, Hall WJ, Cannom DS, et al. MADIT-CRT Trial Investigators. Cardiac-resynchronization therapy for the prevention of heart-failure events. N Engl J Med 2009;361:1329–38.
4. Cheong BY, Muthupillai R, Wilson JM, et al. Prognostic significance of delayed-enhancement magnetic resonance imaging: survival of 857 patients with and without left ventricular dysfunction. Circulation 2009;120:2069–76.
5. Heidary S, Patel H, Chung J, et al. Quantitative tissue characterization of infarct core and border zone in patients with ischemic cardiomyopathy by magnetic resonance is associated with future cardiovascular events. J Am Coll Cardiol 2010;55:2762–8.
6. Roes SD, Borleffs CJ, van der Geest RJ, et al. Infarct tissue heterogeneity assessed with contrast-enhanced MRI predicts spontaneous ventricular arrhythmia in patients with ischemic cardiomyopathy and implantable cardioverter-defibrillator. Circ Cardiovasc Imaging 2009;2:183–90.
7. Wijnmaalen AP, van der Geest RJ, van Huls van Taxis CF, et al. Head-to-head comparison of contrast-enhanced magnetic resonance imaging and electroanatomical voltage mapping to assess post-infarct scar characteristics in patients with ventricular tachycardias: real-time image integration and reversed registration. Eur Heart J 2011;32:104–14.
8. Perez-David E, Arenal A, Rubio-Guivernau JL, et al. Noninvasive identification of ventricular tachycardia-related conducting channels using contrast-enhanced magnetic resonance imaging in patients with chronic myocardial infarction: comparison of signal intensity scar mapping and endocardial voltage mapping. J Am Coll Cardiol 2011;57:184–94.
9. Kellman P, Arai AE, McVeigh ER, Aletras AH. Phase-sensitive inversion recovery for detecting myocardial infarction using gadolinium-delayed hyperenhancement. Magn Reson Med 2002;47:372–83.
10. Haber AM, Schoenberg SO, Hayes C, et al. Phase-sensitive inversion-recovery MR imaging in the detection of myocardial infarction. Radiology 2005;237:854–60.
11. Tseng WY, Liao TY, Wang JL. Normal systolic and diastolic functions of the left ventricle and left atrium by cine magnetic resonance imaging. J Cardiovasc Magn Reson 2002;4:443–57.
12. Yan AT, Shayne AJ, Brown KA, et al. Characterization of the peri-infarct zone by contrast-enhanced cardiac magnetic resonance imaging is a powerful predictor of post-myocardial infarction mortality. Circulation 2006;114:32–9.
13. Assomull RG, Prasad SK, Lyne J, et al. Cardiovascular magnetic resonance, fibrosis, and prognosis in dilated cardiomyopathy. J Am Coll Cardiol 2006;48:1977–85.
14. Yokota H, Heidary S, Katikireddy CK, et al. Quantitative characterization of myocardial infarction by cardiovascular magnetic resonance predicts future cardiovascular events in patients with ischemic cardiomyopathy. J Cardiovasc Magn Reson 2008;10:17.
15. Wu KC, Weiss RG, Thiemann DR, et al. Late gadolinium enhancement by cardiovascular magnetic resonance heralds an adverse prognosis in nonischemic cardiomyopathy. J Am Coll Cardiol 2008;51:2414–21.
16. Kwon DH, Halley CM, Carrigan TP, et al. Extent of left ventricular scar predicts outcomes in ischemic cardiomyopathy patients with significantly reduced systolic function: a delayed hyperenhancement cardiac magnetic resonance study. J Am Coll Cardiol Img 2009;2:34–44.
17. Bernhardt P, Stiller S, Kottmair E, et al. Myocardial scar extent evaluated by cardiac magnetic resonance imaging in ICD patients: relationship to spontaneous VT during long-term follow-up. Int J Cardiovasc Imaging 2011;27:893–900.
18. Schmidt A, Azevedo CF, Cheng A, et al. Infarct tissue heterogeneity by magnetic resonance imaging identifies enhanced cardiac arrhythmia susceptibility in patients with left ventricular dysfunction. Circulation 2007;115:2006–14.
19. Kelly P, Ruskin JN, Vlahakes GJ, Buckley MJ Jr., Freeman CS, Garan H. Surgical coronary revascularization in survivors of prehospital cardiac arrest: its effect on inducible ventricular arrhythmias and long-term survival. J Am Coll Cardiol 1990;15:267–73.
20. Brugada J, Aguinaga L, Mont L, et al. Coronary artery revascularization in patients with sustained ventricular arrhythmias in the chronic phase of a myocardial infarction: effects on the electrophysiologic substrate and outcome. J Am Coll Cardiol 2001;37:529–33.
21. Desjardins B, Crawford T, Good E, et al. Infarct architecture and characteristics on delayed enhanced magnetic resonance imaging and electroanatomic mapping in patients with postinfarction ventricular arrhythmia. Heart Rhythm 2009;6:644–51.
22. de Bakker JM, van Capelle FJ, Janse MJ, et al. Reentry as a cause of ventricular tachycardia in patients with chronic ischemic heart disease: electrophysiologic and anatomic correlation. Circulation 1988;77:589–606.
23. de Bakker JM, Coronel R, Tasseron S, et al. Ventricular tachycardia in the infarcted, Langendorff-perfused human heart: role of the arrangement of surviving cardiac fibers. J Am Coll Cardiol 1990;15:1594–607.
24. Arenal A, del Castillo S, Gonzalez-Torrecilla E, et al. Tachycardia-related channel in the scar tissue in patients with sustained monomorphic ventricular tachycardias: influence of the voltage scar definition. Circulation 2004;110:2568–74.
25. Hsia HH, Lin D, Sauer WH, Callans DJ, Marchlinski FE. Anatomic characterization of endocardial substrate for hemodynamically stable reentrant ventricular tachycardia: identification of endocardial conducting channels. Heart Rhythm 2006;3:503–12.

Key Words: conductive channel ■ congestive heart failure ■ magnetic resonance image.